

A method for rapidly screening functionality of actin mutants and tagged actins

Heidi Rommelaere^{1*}, Davy Waterschoot¹, Katrien Neiryck¹, Joël Vandekerckhove¹ and Christophe Ampe¹

¹Flanders Interuniversity Institute for Biotechnology (VIB 09) and Department of Biochemistry, Faculty of Medicine and Health Sciences, Ghent University, B-9000 Gent, Belgium.

*To whom correspondence should be addressed: Heidi Rommelaere, Flanders Interuniversity Institute for Biotechnology (VIB 09) and Department of Biochemistry, Faculty of Medicine and Health Sciences, Ghent University, B-9000 Gent, Belgium. Phone: 32 9 264 93 33; Fax: 32 9 264 94 88; Email: Heidi.Rommelaere@ugent.be

Submitted: February 18, 2004; Revised: September 23, 2004; Accepted: October 1, 2004; Published: October 25, 2004.

Indexing terms: Actins; Binding sites; Protein folding.

ABSTRACT

Recombinant production and biochemical analysis of actin mutants has been hampered by the fact that actin has an absolute requirement for the eukaryotic chaperone CCT to reach its native state. We therefore have developed a method to rapidly screen the folding capacity and functionality of actin variants, by combining *in vitro* expression of labelled actin with analysis on native gels, band shift assays or copolymerization tests. Additionally, we monitor, using immuno-fluorescence, incorporation of actin variants in cytoskeletal structures in transfected cells. We illustrate the method by two examples. In one we show that tagged versions of actin do not always behave native-like and in the other we study some of the molecular defects of three β -actin mutants that have been associated with diseases.

INTRODUCTION

Actin is the major component of the microfilament system of eukaryotic organisms and plays a central role in cell motility processes. Therefore it interacts with itself and with a broad array of actin binding proteins (ABPs) that regulate its polymerization (reviewed in (1)). Additionally, actin requires the help of the molecular chaperones CCT and prefoldin to adopt a properly folded state (2-4). *In vitro* characterization of naturally occurring disease-causing actin mutants (e.g. the α -actin mutants causing nemaline myopathy, (5)) and studies of interactions of actin and its partner proteins often require the generation of mutant actins. However, recombinant production and purification of actin

mutants for biochemical studies is a laborious process (e.g. 6-8) and not possible in bacteria, since the bacterial chaperonin analogue GroEL (9) is incapable of productively folding actin (10). Moreover, we have shown, that introducing mutations in β -actin can result in an unfolded, not-functional molecule (11). Consequently, there is need for a method to rapidly check if an actin variant is functional, before going through the effort of expression and purification. The method we here present fulfils this need and additionally allows gaining some biochemical insight in the behaviour of actin variants. It originates from our work on monitoring the folding capacity and functionality of actin and artificial actin mutants and consists of analysing ³⁵S-labeled actins, produced in reticulocyte lysate, via native gel electrophoresis, bands shift assays and copolymerization tests in

addition to transfection in cultured cells (11). The use of the method is illustrated by two examples: 1) we investigate the influence of adding tags to actin on its functionality, and 2) we characterise three disease associated β -actin mutants.

The first example was chosen to check if tagged proteins behave native-like, which is an important issue, considering that the use of tagged proteins became very popular in recent years. Tags like GST or HIS are generally added to facilitate purification of proteins, and in this case systems have been developed to remove the tag. This avoids having the tag interfere with the function of the protein of interest (reviewed in (12)). On the other hand, tags like GFP, myc or FLAG are added with the aim of visualising transfected proteins inside cultured cells. For most tags, cells have to be fixed and stained with an antibody against the tag. GFP-tagging however offers the advantage that it can be observed in living cells (13). Since the tags are essential for the visualization of the protein under investigation, they cannot be removed and consequently it is possible tags may interfere with the protein's cellular activity and we show here that this is indeed the case for human β -actin molecules tagged with GFP at the N-terminus or with a myc-tag at the C-terminus.

In the second example, we employ our assay on three clinical β -actin isolates: R28L and G245D, both associated with tumorigenesis (14, 15) and E364K, discovered in a patient with neutrophil dysfunction (16). Actin R28L (also called beta m-actin) was isolated from a low metastatic B16 melanoma mouse cell line. Its expression however disappears or is very low in highly metastatic B16-F10 cell lines (17). Introduction of the mutant in these cells even reduces invasiveness and metastatic ability (14, 18). G245D was isolated from a tumorigenic human fibroblast cell line (HuT-14) (19). When HuT-12 fibroblasts transfected with this mutant and expressing high levels of it, are introduced in athymic mice, subcutaneous tumours are generated and the expression of tropomyosins is elevated (20). E364K was expressed together with normal β -actin in a female patient suffering from recurrent infections, photosensitivity and mental retardation. She had also abnormalities in neutrophil chemotaxis (a process connected to actin), superoxide production and membrane potential response (16). Using our assays, we could not find any defect for R28L, but G245D shows decreased binding to the eukaryotic chaperonin CCT. E364K on the other hand, displays increased CCT and prefoldin binding and little protein is released in a correctly folded state.

MATERIALS AND METHODS

Construction of the β -actin mutants

β -actin mutants were made with the Quik Change site directed mutagenesis kit (Stratagene) as described in Rommelaere *et al.* (11). N-terminal myc-tagged wild type and actin mutants were made by PCR starting from the appropriate actin cDNA in the pcDNA3.1 vector (Invitrogen) using a 5' primer containing the myc-coding sequence, preceded by a HindIII site and followed by an KpnI/Nco I site and a 3' primer containing a XbaI site.

After restriction these fragments were ligated in HindIII-XbaI digested pcDNA3.1.

N-terminal GFP-tagged actins were made from their myc-tagged versions by excision of the myc-tag coding sequence with Hind III and KpnI, and replacing it by the GFP cDNA equipped with a linker (coding for SGLRSVPT) which had previously been PCR amplified using a 5' primer containing a HindIII site and a 3' primer containing a KpnI site. C-terminally myc-tagged actins were made by cloning them in the pcDNA3.1/CMycA-vector using KpnI and XbaI. These constructs were sequenced at the 5' and /or 3' end of their coding sequence.

Expression of actin mutants and band shift assays with actin binding proteins

We expressed the actin mutants as ^{35}S -labeled proteins in *in vitro* transcription translation reactions in reticulocyte lysate (Promega, for details see step-by-step protocols). After 1h30 of reaction, we determined the amount of ^{35}S -actin in the various complexes by analysing the reaction products on non-denaturing gels, either with or without 200 μM ATP (21), and the total amount of expressed protein by analysis on denaturing SDS- (22) or tricine-gels (23) followed by autoradiography and quantification by Phosphor imager analysis (Typhoon 9200 variable mode imager, Amersham Biosciences) and the ImageQuant software package. The analysis on denaturing gels is also important to check if the produced protein has the correct length. Actin is known to be proteolytically sensitive at its C-terminus (24), but only very minor degradation is observed for *in vitro* produced actin variants indicating that protease activity in reticulocyte lysates is low.

For the band shift assays, 1 μl of the respective actin binding proteins was added to 3 μl of an *in vitro* transcription translation reaction. After 1 minute incubation, the mixture was analysed on native gels with 200 μM ATP. The final concentration of the respective actin binding proteins was 12.5 μM for thymosin β_4 , 13 μM for profilin IIa, 2 μM for DNase I and 1 μM for VDBP. These concentrations are the minimal amounts of the actin binding proteins needed to cause a band shift of wild type actin, as was determined by a concentration series (data not shown).

DNase I was purchased from Worthington and VDBP from Calbiochem. Thymosin β_4 was chemically synthesized on a model 431A peptide synthesizer using solid phase Fmoc chemistry. Recombinant profilin-IIa was purified according to Lambrechts *et al.* (25).

Time course experiments

After 6 minutes of incubation of an *in vitro* transcription/translation reaction of actin or actin mutant G245D an excess of cold methionine (0.9 mM final concentration) was added. Aliquots of 5 μl were taken 6, 9, 12, 15, 18, 21, 30, 45, 60 and 90 minutes after chasing, and put on ice to stop the reaction. 3 μl was analysed on a native gel with ATP to quantify the amount of CCT-bound and released actin and 1

μ l on a denaturing tricine gel (23), to quantify the total amount produced actin. The relative amount of CCT-bound and released actin for each time point was plotted on a graph.

Copolymerization assays

25 μ l of an *in vitro* transcription translation reaction of wild type or mutant β -actin was centrifuged at 100,000 rpm in a Beckman airfuge to remove aggregates. To the supernatant, we added 25 μ l of 12 μ M α -actin in G-buffer (2 mM TrisHCl, pH 8, 0.2 mM CaCl₂, 0.5 mM DTT, 0.2 mM ATP), to drive actin polymerization. This actin was purified from rabbit skeletal muscle according to Pardee *et al.* (26). This protocol includes gel filtration, whereby the cross-linked actin dimers, produced during the acetone extraction step (27), are removed. Note that α - and β -actin isoforms are able to form copolymers (28).

We adjusted the buffer conditions to 100 mM KCl and 1 mM MgCl₂ (F-buffer) and allowed the actin to polymerise for 2 hours at room temperature. F-actin was pelleted by centrifugation at 100,000 rpm for 20 minutes (= pellet 1). The supernatant (sn1) was removed, the pellet washed and resuspended in 80 μ l G-buffer. Actin was allowed to depolymerise overnight at 4°C. A second round of polymerization was induced for 2 hours. F-actin was pelleted by centrifugation at 100 000 rpm for 20 minutes (= pellet 2) and separated from the supernatant (sn2). Aggregates, sn1, sn2 and pellet 2 were analysed on a 12.5% SDS-gel followed by autoradiography. The amount of ³⁵S-labeled actin in each fraction was quantified using phosphor imaging. All mutants were analysed at least three times.

In vivo localization

We transfected pcDNA3.1 vectors encoding GFP- or myc-tagged β -actin (wild type or mutant) in NIH 3T3 fibroblast cells using electroporation or lipofectamin 2000 (BD Biosciences, Clontech). 24 hours after transfection, cells were washed with PBS and fixed with 3% paraformaldehyde, permeabilized with 0.1% Triton X100 in PBS and incubated for 1 hour at room temperature with phalloidin-alexa-red (Molecular Probes) and anti-myc-FITC antibody in the case of myc-tagged actin (Invitrogen). Stained cells were examined using a Zeiss Axioplan II epifluorescence microscope equipped with a X40 objective or an Olympus IX71 epifluorescence microscope equipped with a X100 objective. Images were taken using respectively a cooled CCD Axiocam Camera and KS100 software (Zeiss) or a cooled Spot Camera (Diagnostic Instruments) and Analysis software (Soft Imaging Systems).

RESULTS AND DISCUSSION

Native gel analysis and band shift assays for *in vitro* expressed actin

The method we describe here consists of analysing ³⁵S-labeled actins produced by *in vitro* transcription/translation in

reticulocyte lysate, which endogenously contains the actin folding machines prefoldin and CCT (2, 4). As a follow-up we often transfect these variants in cultured cell lines. To combine these methods efficiently, it is necessary to clone the actin variants in a vector that possesses a T7 or SP6 promoter (for expression in reticulocyte lysate) and a promoter that allows expression in cultured cells. We found the pcDNA3.1 vector, containing a T7 and a P_{CMV} promoter, very suitable for this purpose.

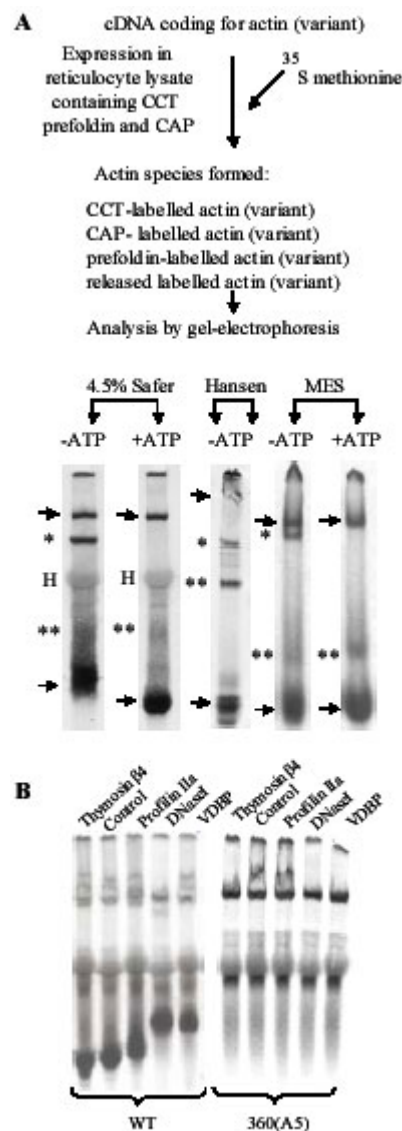


Fig. 1: Actin-complexes have different mobilities on different native gels. (A) Outline of the production and electrophoretic analysis of ³⁵S-actin (variants) in reticulocyte lysate. Comparison of analysis on Safer (21), Hansen (34, 59) and MES-gels (2). The upper arrows indicate CCT-actin, the lower arrows released actin, * indicates CAP-actin, ** prefoldin-actin and H haemoglobin. (B) Autoradiogram of discontinuous 4.5% - 7.5% Safer gels showing band-shift assays for WT-actin and the actin mutant 360(A5). The latter is released from CCT but not folded, since it does not bind to any ABP tested. For WT-actin, thymosin B4 causes a small downward shift and profilin IIa a small upward shift.

The *in vitro* expressed ³⁵S-labeled actin variants are analysed in various ways: on denaturing or native gels, in a band shift assay or in a copolymerization test. Analysis on denaturing SDS- or

tricine-gels followed by autoradiography is necessary to estimate the total amount of expressed protein and to check if the produced protein has the correct length. More accurate quantification can be obtained with phosphor imaging. Native gel analysis is performed in the presence or absence of ATP. It reveals the various actin complexes during its folding process, i.e. actin associated with CCT, actin associated with prefoldin and released actin (Fig. 1A). In some cases, the latter band is not observed, which means that the particular actin variant remains arrested on CCT and is not able to fold (11). In the absence of ATP an additional complex of actin-CAP can be observed. CAP is also endogenously present in reticulocyte lysates (29) and has a high affinity for the nucleotide free state of actin (11). Note that the actin band in gels without ATP has the tendency to smear. During electrophoresis some of the actin molecules loose their bound ATP (originating from the transcription/translation reaction) and since actin needs this nucleotide for its stability (30), this part of the population denatures.

To check if the released actin is correctly folded, we perform band shift assays, previously developed by others (e.g. (21, 31)). In these assays we test if the actin variant is able to bind to a panel of ABPs that contact different surfaces of the actin molecule, in this case thymosin β 4, profilin IIa, DNase I and VDBP (Fig. 1B). An upward or downward shift of the released actin species on native gels indicates binding. No binding to the majority of these proteins indicates that the released actin is incorrectly folded (see e.g. mutant 360(A5)* in Fig. 1B). If binding to only one of these proteins is abolished, it indicates that actin is changed in a region important for binding to this partner ((11), see also below). Also relatively weak interactions (i.e. thymosin β 4 mutants: Kd 100 μ M) can be monitored using this assay (32). We assume this is because during electrophoresis, high local concentrations of proteins are generated when moving towards the same pole (i.e. proteins with acidic pI's to the anode) because of stacking. Indeed, a problem occurs when analysing proteins with a basic pI and high off rates. This is for example the case for one of the profilin isoforms. Profilin I and IIa have a similar Kd for actin (0.4 and 0.7 respectively, (25)). However, no complexes between profilin I (pI 8.46) and actin can be detected because this basic isoform migrates towards the cathode and out of the gel, whereas complexes with the more acidic isoform, profilin IIa (pI 6.55), can be observed. Cofilin, which has also a basic pI (8.22), but slightly lower than the one of profilin I, can migrate into native gels (33), which indicates that small differences in pI can have a great impact on the migration direction. Obviously this is linked to the pH at which electrophoresis is performed. This is in turn dependent on the temperature because the pKa-values of buffers (and especially of TRIS) change with temperature.

As outlined above, native or non-denaturing polyacrylamide gels are used to analyse native proteins or protein-complexes. The migration of these proteins depends on their size, shape and charge and, as already mentioned, on the pH maintained during gel electrophoresis. Therefore a careful choice of the buffer system and of the acrylamide concentration of the gel is required, depending on the type of analysis. In our case for example, 4.5%

Safer gels at pH 8.7 (21) are best suited to analyse and quantify actin folding and actin binding to CCT and CAP (Fig. 1A). To perform actin band shifts however, it is more adequate to use discontinuous 4.5% - 7.5% or 4.5% - 10% Safer gels (Fig. 1B). The upper 4.5% part of the gel prevents aggregation of the native actin when it enters the gel, whereas in the lower part, the higher acrylamide concentration compresses the protein bands, which facilitates judging the occurrence of a band shift. To analyse and quantify prefoldin-actin complexes however, 6%-13% discontinuous native gels at pH 7 according to Hansen *et al.* (34) are preferred, since they produce a sharp prefoldin-actin band (35) in contrast to Safer gels, where this band is rather diffuse. However Hansen gels are not suited to quantify actin-CCT complexes (Fig. 1A).

Reticulocyte lysate contains large amounts of haemoglobin and this may disturb the electrophoresis. Therefore we never load more than 3 μ l reticulocyte lysate/well on a mini-gel with ten lanes, and even then haemoglobin appears as a thick spot at approximately one third of the gel (see e.g. Fig. 1A) and in some cases this band is exactly at the position of the protein complex to analyse (e.g. actin-GroEL, (36)). In this case MES-gels with a pH of 6.7 exactly should be used. At this pH, haemoglobin does not enter the gel, whereas the actin-complexes do (Fig. 1A).

All these examples illustrate that, depending on the protein and the application, electrophoresis conditions have to be carefully chosen and as much as possible standardized.

*Note: Actin 360(A5) means that amino acids 360 to 364 of actin are changed to alanine (11).

Tests for copolymerization capability of actin variants

Another important feature of actin is its self-association capability, hence it is necessary to test if actin variants are still able to polymerise (the experimental outline is presented in Fig. 2A). Since the combined amount of endogenous actin and produced actin (mutant) in reticulocyte lysates, is limited, we are obliged to add wild-type carrier actin to induce polymerization. With respect to the carrier actin, we use rabbit α -skeletal actin, since this actin is easy to purify, possesses all correct post-translational modifications and forms mixed polymers with other actin isoforms (28). The use of this actin has however the drawback that one always has to include the WT non-muscle isoform as a control when analysing non-muscle actin variants and one can only estimate relative copolymerization capacities. But even when analysing α -skeletal muscle actin mutants it is very important to include in every test series a control with the wild type isoform. This is to account for differences in quality of the carrier actin and variability of different batches of reticulocyte lysates. The latter also results in variability of concentrations of the ABPs present in the lysate that may influence the critical monomer concentration and may sequester a population of the actin monomers. Comparison with the WT isoform however overcomes all these inconveniences.

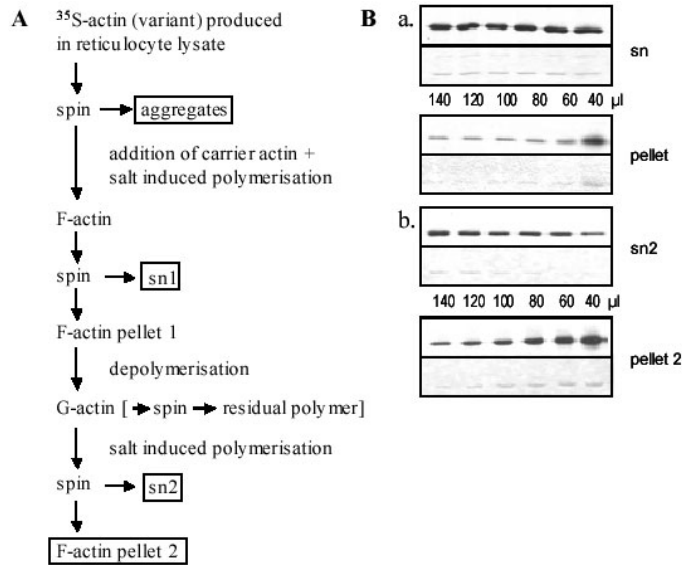


Fig. 2: Outline and optimization of copolymerization tests. (A) Outline of the copolymerization assay for ³⁵S-actin (variants) produced in reticulocyte lysate. The fractions that we analyse via SDS-PAGE are boxed. An extra spin of the depolymerized F-actin pellet 1 to remove residual polymer is optional (see comments in protocol) but was not performed in the present study. (B) Test to determine the optimal volume for depolymerisation of actin in the copolymerization assay. Samples of *in vitro* transcription translation reactions and α -actin from rabbit skeletal muscle were mixed, induced to polymerise and pelleted. This pellet was solubilized in G-buffer in the indicated volumes and depolymerized overnight, and divided in two. One half was left unchanged (a), the other half was induced to polymerise by addition of salts (b). These two fractions were centrifuged and for both, supernatants and pellets were analysed on 12% SDS-gels. The upper panels show the autoradiograms, the lower panels the corresponding Coomassie stained gels. This test shows that the optimal volume for repolymerization at the actin concentration used in this assay is 80 μ l (b) and that this volume is also sufficient for depolymerization (a).

Prior to induction of polymerization, it is necessary to remove aggregates by high-speed centrifugation. This is particularly relevant when dealing with unstable actin mutants. After the first polymerization round, the F-actin polymers are pelleted by spinning at high speed and depolymerized, where after a second round of polymerization is initiated and F-actin pelleted again. Two rounds of polymerization are necessary to avoid unspecific binding of the actin variants to the filaments. Indeed there are ABPs present in the reticulocyte lysate that may associate with the filaments. By performing the second polymerization round these ABPs are diluted out (compare for instance the presence of additional protein bands on the Coomassie stained gels of sn2 and pellet 2 in Fig. 6A). This is important if this particular ABP has two actin binding sites through, which an actin variant can indirectly associate with filaments.

The amount of (mutant) actin in each fraction is then measured after SDS-PAGE by counting ³⁵S either in the initial spin (aggregates) before addition of carrier actin and induction of polymerization, or in the supernatants (sn1 and sn2, containing G-actin) of the two high speed spins following polymerization, or in the final pellet (pellet 2, containing F-actin) as outlined in the protocol section and in Fig. 2A (see also below Fig. 3E and 6B).

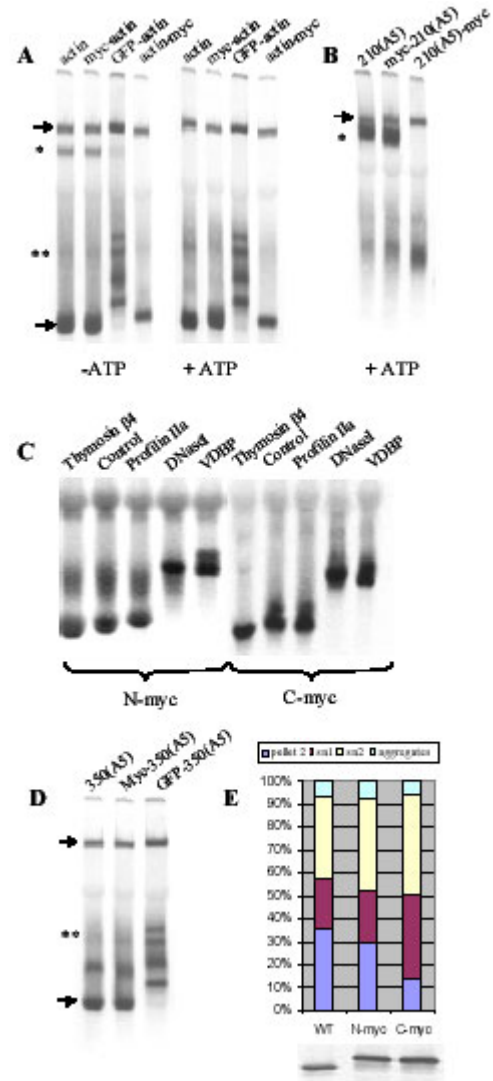


Fig. 3: Native gel analysis of differently tagged actins reveals a different behaviour. (A-D) Autoradiograms of native gels of ³⁵S-labeled GFP- and myc-tagged β -actin and mutants produced in *in vitro* transcription translation reactions. (A) WT β -actin in the absence (left) or presence (right) of ATP. (B) β -actin mutant 210(A5) in the presence of ATP. (C) Band-shift assay of N-terminally (left) or C-terminally (right) myc-tagged WT β -actin. Only the lower part of the gel is shown. (D) β -actin 350(A5) in the presence of ATP. The upper arrows indicate CCT-actin, the lower arrows released actin, * indicates CAP-actin, ** prefoldin-actin. (E) Copolymerization of β -actin compared to myc- β -actin (N-myc) and β -actin-myc (C-myc). Samples of *in vitro* transcription translation reactions and α -actin from rabbit skeletal muscle were mixed, induced to polymerise and pelleted. The amount of ³⁵S-labeled actin in aggregates, supernatants (sn1 and sn2) and pellet 2 (see Fig. 2A) were calculated after analysis on 12.5 % SDS-gels. One such a gel is shown below the graph, it also indicates that only minor cleavage at the C-terminus of actin occurs in lysate.

We have tested various conditions to derive the most suitable parameters to perform the depolymerization and second polymerization step. Initially, we depolymerized actin pellet 1 by resuspending it in 500 μ l G-buffer to assure complete depolymerization. To then re-establish the critical concentration for the second round of polymerization, one needs to concentrate the actin solution to +/- 50 μ l using Microcon 10 concentrators. However, the concentrator membranes bind significant amounts of actin. Therefore we tried to avoid

concentration and searched for a balance between the minimal volume for depolymerization and the maximal volume for the second polymerization. Pellet 1 was solubilized in G-buffer in the volumes indicated in Fig. 2B and depolymerized overnight. One half of this reaction was left unchanged and the other induced for polymerization. After ultracentrifugation supernatants and pellets were analysed on 12% SDS-gels. The optimal volume for repolymerization is 80 μ l at the carrier actin concentration used in this assay.

We want to emphasise here that this assay only reveals the capacity of mutant actin to copolymerise with carrier actin. For detailed kinetic studies on the polymerization behaviour of mutants, or for clinically relevant copolymerization assays (e.g. 50% disease related mutant with 50% WT-actin) recombinant expression and purification of the mutant actin is superior. For this purpose yeast can be used, although this recombinant actin is not completely post-translationally modified (e.g. not methylated at H73, 37) and a recent paper shows successful baculovirus expression of actin (38). However recombinant production in this manner is not trivial and cannot yet easily be done for a large panel of actin mutants. Therefore the method, described above, should also be viewed as a screening tool for choosing which mutants to express recombinantly and as a quality control, i.e. does the mutant fold properly? The latter is illustrated below where we investigate the influence of tags on the functionality of actin.

Tags may interfere with the functionality of actin variants; also the location of the tag is of importance

Since wild type actin gets incorporated in stress fibers after introduction in cultured cells (39), the effect of actin mutations is often tested *in vivo* by transfection of tagged actin mutants. Staining for the tag and co-staining with phalloidin allows monitoring if the actin variant is incorporated in the actin cytoskeleton or if it forms aberrant structures. It can indeed happen that a mutant with normal copolymerization capacity *in vitro*, behaves abnormally in the cellular context (e.g. α -actin mutant H40Y in (40)). Various tags either at the N- or C-terminus of actin have been used to perform transfection and transformation experiments (e.g. 41-43). However many actin binding proteins interact at the bottom of subdomains 1 and 3 of actin (see Fig. 5A, (44)). Since the C- and N-terminus of actin are both located in subdomain 1, this is in the neighbourhood where tags will be located. Consequently, it is possible that these tags will interfere with binding of actin binding partners and perturb actin function when transfected in cells, alternatively tags may interfere with the folding machinery. For this reason we find it necessary to investigate the behaviour of tagged actin variants in the *in vitro* system described above prior to transfecting actin variants in NIH fibroblasts. We compare the use of small and larger tags, also paying attention to their site of fusion.

We first describe the effects of fusing the short myc-tag to respectively the N- and the C-terminus of actin. N- and C-terminally myc-tagged actins behave completely like WT actin on

native gels in the presence of ATP with respect to folding (Fig. 3A). However, in the absence of ATP, no CAP-binding is observed for actin-myc. We have previously shown that actin mutant 210(A5) tightly binds to CAP, even in the presence of ATP (11). Despite this we observe no CAP-binding when this mutant has myc on the C-terminus (Fig. 3B). Similarly, when the binding capacity of actin-myc to thymosin β 4, profilin IIa, DNase I and VDBP was tested, no shift was seen in the case of profilin IIa. These results indicate that the tag at this position interferes strongly with wild type actin function (Fig. 3C). Actin-myc also incorporates less in actin polymers *in vitro* (Fig. 3E) and when transfected in NIH3T3 fibroblasts, it accumulates in abnormal protrusions that stain with phalloidin, but it does not incorporate in actin stress fibers (Fig. 4A). Myc-actin however copolymerises quasi normally and incorporates nicely in stress fibers (Fig. 4A).

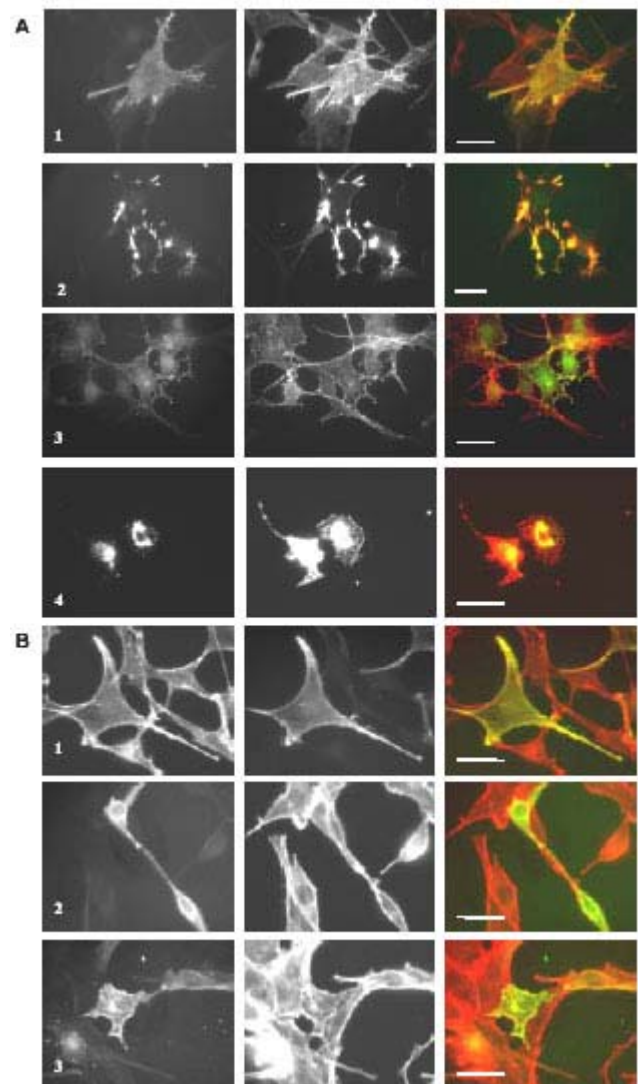


Fig. 4: Expression of GFP-tagged actin and mutants in NIH 3T3 cells gives a different picture than expression of the myc-tagged versions. (A) β -actin, 1. N-terminally myc-tagged, 2. C-terminally myc-tagged, 3 and 4. N-terminally GFP-tagged. (B) β -actin 350(A5), 1. N-terminally myc-tagged, 2. and 3. N-terminally GFP-tagged. Left panels are phalloidin staining of filamentous actin, middle panels, anti-myc-FITC staining or GFP-fluorescence of the expressed variants, right panels overlay (phalloidin: red; myc/GFP: green). Scale bar is 40 micrometer.

So we conclude that N-terminally myc-tagged actin behaves like non-tagged actin in our assays, whereas a C-terminal myc-tag interferes with *in vitro* and *in vivo* copolymerization, CAP and profilin IIa binding. Thus a tag on the N-terminus is preferable, as was also found for tagged ACT88F actin in *Drosophila* (43), although we cannot rule out that it will interfere with myosin binding, since myosin has been predicted to interact with the N-terminus of actin (45). Interaction with filament binding proteins is however difficult to probe with our method, given the low concentrations of mutant actins produced in reticulocyte lysates.

Since in some cases monitoring of living cells is required, we tested also the influence of a GFP-tag. We added this tag only at the N-terminus since even the smaller myc-tag interferes with functionality when fused to the C-terminus. Analysis on native gels reveals four discrete bands, of which only the lower one is representing folded actin, since it is the only band that shifts with our ABP cassette (Fig. 3A and data not shown). The identity of the other bands is presently unknown; one may represent prefoldin-actin and the two others not functional or incorrectly folded species. Indeed the fact that the CCT-binding of GFP-actin is increased indicates this mutant has difficulties to fold properly and thus only a minor part of the GFP-actin reaches a functional form. Since this population also does not interact with CAP, it indicates that the GFP-moiety at the N-terminus also may interfere with other actin functions. When this GFP-actin is transfected in fibroblasts, we observe in half of the cells a partial incorporation in stress fibers (a significant amount of GFP-actin is not incorporated in stress fibers compared to myc-actin transfected cells), but in the others, aggregates are formed (Fig. 4A). Probably in the latter case, the not correctly folded species are predominantly formed. The same phenomenon is observed with actin mutants. N-terminally myc-tagged actin 350(A5) for example, folds correctly (Fig. 3D) and incorporates in stress fibers in NIH3T3 cells, however the GFP-version of it, again is partly folded and in half of the cases does not integrate in stress fibers in transfected cells (Fig. 4B).

In conclusion, our results show that a tagged actin does not necessarily behave similar to the non-tagged version. Therefore, we advise to monitor folding and functionality by native gel analysis of *in vitro* expressed labelled actins, as presented here. Obviously, this may also apply to other tagged proteins; for instance C-terminal tagged versions of profilin IIa have a dramatically reduced affinity for proline-rich sequences whereas their affinity for actin appears normal (46). In these cases other assays that are standard for the protein of interest can be used. This will give more credit to data based on transfection of tagged proteins in cultured cells, where tags may serve to visualise the target proteins or as bait for immuno-precipitations. In particular for the latter application a quality control may be necessary because this technique is presently being used for high-throughput mapping of protein-protein interactions using e.g. mass spectrometry (47).

Analysis of the disease associated β -actin mutants R28L, G245D and E364K reveals some of their molecular defects

As a second illustration of our method, we characterized three disease associated β -actin point mutants. One is associated with neutrophil dysfunction (E364K) and two are connected to tumorigenesis (G245D and R28L). As can be seen on the 3D-representation of actin (Fig. 5A, (48)), these mutations are dispersed in the 3D-structure, G245D is at the top of subdomain 4, E364K at the right bottom of subdomain 1, while R28L is at the junction of subdomain 1 and 2. Native gel analysis shows that all three mutants are capable of folding, however the amount of folded protein in the case of E364K is severely reduced and the majority of the protein remains bound to CCT and prefoldin, or is aggregated (Fig. 5B). Also CAP binding is lost. This suggests this mutant is folding compromised or unstable. For R28L, the CAP binding is reduced. Since G245D is located in the middle binding region for CCT (36), and given that actin mutant 245(A5) is compromised in CCT-binding (Fig. 5C), and that the β -actin mutant G245A shows decreased CCT-binding (29), we investigated also the CCT-binding capacity of this mutant. Therefore we introduced this mutation in an actin variant, which lacks the first six amino acids and is folding compromised, as relative CCT-binding can only be reliably quantified when no folded protein is released (36). Indeed G245D shows decreased binding to the eukaryotic chaperonin CCT (Fig. 5C).

The *in vitro* expression system also allows monitoring the kinetics of CCT-actin complex formation and folding, by performing time course pulse chase experiments. By adding cold methionine six minutes after initiation of the reaction, one can follow the fate of the molecules that are labelled in the first six minutes. In the case of G245D, it shows that this mutant accumulates in the initial phase less on CCT than wild type actin, but finally reaches a similar amount of folded actin, suggesting this mutant is synthesized more slowly than wild type actin (Fig. 5D).

To test if the three mutants are correctly folded, we performed band shift assays with our ABP panel (Fig. 5E). The fact that all mutants shift with all tested proteins indicates they are correctly folded, however with our assay it is difficult to detect subtle differences in the affinity of the mutants for the ABPs (see also (11)). One would indeed expect a decreased affinity of E364K for profilin, since E364 is involved in a salt bridge with K125 of profilin I (49) and a decreased binding has been reported by Nunoi *et al.* (16), however the same mutation in the indirect flight muscle-specific *Act88F* actin of *Drosophila melanogaster* results in increased binding to profilin (7).

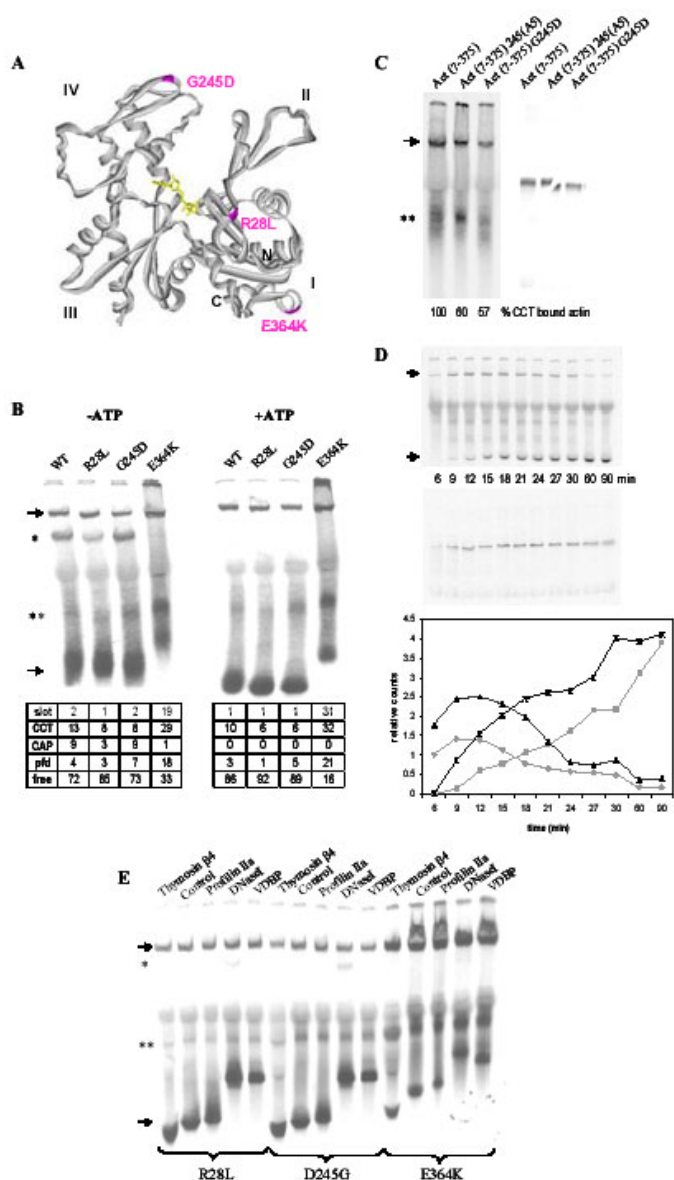


Fig. 5: The β -actin mutants R28L, G245D and E364K fold and bind to the tested ABPs, however G245D shows decreased binding to CCT and E364K is not efficiently released by CCT and prefoldin. (A) Ribbon representation of the actin fold (48) with the positions of the mutations R28L, G245D and E364K indicated in pink. ATP is in yellow. (B) Autoradiogram of a native gel analysis in the presence (right) or absence (left) of ATP of 35 S-labeled β -actin and mutants R28L, G245D and E364K produced in an *in vitro* transcription translation reaction. Note that the lower mobility of E364K is due to the charge inversion. The upper arrow indicates CCT-actin, the lower arrow released actin, * indicates CAP-actin, ** prefoldin-actin. (C) Autoradiogram of a native and a denaturing gel analysis of β -actin(7-375), β -actin(7-375) G245D, and β -actin(7-375) 245(A5). The % CCT-bound actin (arrow) was calculated by dividing the amount of CCT bound target protein (quantified from the native gels), by the total amount of expressed protein, (quantified from the denaturing gels) relative to the 100% binding reference β -actin(7-375) (36). ** indicates prefoldin-actin. (D) Time course pulse chase of β -actin G245D versus WT-actin. Aliquots of 3 μ l of a time course pulse chase reaction for WT β -actin and β -actin G245D were stopped at the given time-points and analysed on a native and a denaturing gel and quantified. The gels represented are for G245D. The upper arrow indicates CCT-actin, the lower folded actin. The relative amounts of CCT-bound and free actin were plotted in function of time. \blacktriangle represents Actin-CCT, * free actin, \blacklozenge G245D-CCT and \blacksquare free G245D. (E) Autoradiogram of a native gel analysis in the presence of ATP of 35 S-labeled β -actin mutants R28L, G245D and E364K produced in an *in vitro* transcription translation reaction (control), band shifted with either thymosin β 4,

profilin IIa, DNase I or VDBP. The upper arrow indicates CCT-actin, the lower arrow released actin, ** indicates prefoldin-actin. We do not know the identity of the band indicated with * in the lanes with DNase I, but it may represent a DNase I-actin-CAP complex.

The next feature of the actin mutants we tested was their ability to copolymerise with purified β -actin (Fig. 6). R28L copolymerises normally and G245D shows a modest reduction in copolymerization capacity. This is not surprising since residue 245 is part of a surface involved in the interaction between actin monomers (50). Studies of polymer formation with only actin mutant G245D, purified after expression in yeast, also show impaired polymerization although different conditions were used (6). E364K was mostly recovered in aggregates and in the supernatant (CCT and prefoldin bound actin remain in the supernatant), which is in agreement with the fact that only a minor fraction of the molecules is folded (see above). This probably results in the reduced amount of this mutant in the filamentous fraction. However Nunoi *et al.* (16), observed no defect in cell free polymerization of this mutant, but since they isolated this mutant from the cytosol fraction it is likely they worked with that population of molecules that was properly folded.

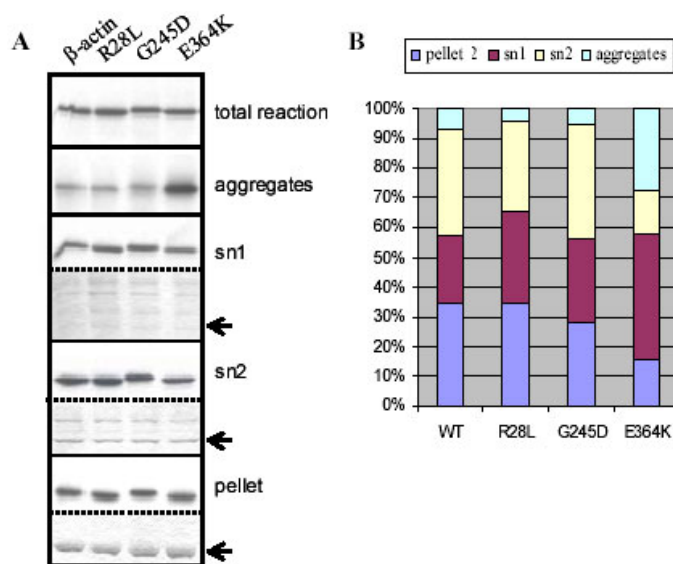


Fig. 6: The β -actin mutants R28L, G245D and E364K are able to copolymerise, although E364K is more prone to aggregation. Samples of *in vitro* transcription translation reactions and α -actin from rabbit skeletal muscle were mixed, induced to polymerise and pelleted. The amount of 35 S-labeled actin in aggregates, supernatants (sn1 and sn2) and pellet 2 (see Fig. 2A) were calculated (B) after analysis on 12.5 % SDS-gels (A). Upper panels are autoradiograms, lower panels the corresponding Coomassie stained gels, the arrow indicates the migration position of actin.

We subsequently investigated whether the mutants could incorporate in actin structures when transfected as N-terminally myc-tagged proteins in NIH3T3 fibroblasts. This was indeed the case for R28L and G245D (Fig. 7A and B) and is in agreement with our *in vitro* results and with previous reports: R28L becomes part of the microfilaments (14, 17); G245D accumulates in stress fibers but does however not participate in the formation of the actin filament-rich perinuclear network (51) and the transfected fibroblasts show altered morphology. In the *Drosophila* Act88F

actin, G245D is antimorphic with regard to flight and causes myofibrillar disruption even in the presence of two normal alleles. It is initially incorporated into myofibrils and later induces their degeneration from centre to periphery (52).

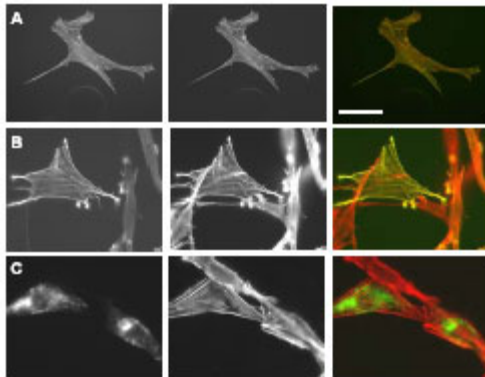


Fig. 7: β -actin R28L and G245D are incorporated in stress fibers in NIH3T3 fibroblasts, whereas E364K resides in aggregates. Myc- β -actin R28L. (B) Myc- β -actin G245D. (C) Myc- β -actin E364K. Left panels are anti-myc-FITC staining of the expressed mutants, middle panels phalloidin staining of filamentous actin, right panels overlay (phalloidin: red, myc: green). Scale bar is 40 micrometer.

In cells transfected with myc-E364K, the mutant actin is not incorporated into stress fibers, but forms aggregates in the cytoplasm (Fig. 7C). This is consistent with a folding defect and agrees with the observation that the E364K mutant induces in *Drosophila* the production of heat shock proteins (53). When it is homozygously expressed in a null strain, no myofibrils are formed, and it is antimorphic for flight ability when expressed in an Act88F null strain together with wild type actin. An amino acid substitution at the identical site in actin molecules of *S. cerevisiae*, E364A, provoked temperature sensitivity (54).

In conclusion, so far we did not find a defect for the β -actin mutant R28L, but for G245D we found decreased CCT-binding and delayed synthesis, suggesting that fewer functional actin is formed in cells. How this can be related to tumour induction still remains a question. Both mutants are able to incorporate in the actin cytoskeleton. E364K on the contrary has an increased CCT and prefoldin binding, it is aggregation sensitive and only little protein is released in a correctly folded state. In cultured cells it is located in aggregates in the cytoplasm. The disease caused by this mutant may be due to a general dysfunction of the actin cytoskeleton.

CONCLUSIONS

We have developed a method to rapidly screen the folding capacity and functionality of actin variants, by combining *in vitro* expression of labelled actins and their analysis via native gels, band shift assays and copolymerization tests. The method can in principle be extended to any other protein that migrates, alone or in complex with a particular partner, into native gels. We already showed the usefulness of this method for characterization of actin mutants (11, 40) and such characterizations are becoming more and more

important since the list of clinical actin mutants that are discovered is growing. In addition to the three disease-related β -actin mutant analysed here, more than sixty α -skeletal muscle actin mutants that cause nemaline myopathy have been isolated (5), four α -cardiac actin mutants that cause cardiomyopathy (55, 56) and recently five γ -actin mutants that are associated with dominant progressive deafness (DFNA20/26) (57, 58). Additionally, using this method, we show that tagged and non-tagged actins do not necessarily behave similarly. Especially the use of tags on the C-terminus of actin as well as GFP-tags has to be avoided. Therefore, we recommend using the analytical method presented here to first check the behaviour of tagged proteins before transfecting them in cells.

ACKNOWLEDGMENTS

We thank Daisy Dewitte for the purification of α -actin. H.R. is a Postdoctoral Fellow supported by the Flanders Interuniversity Institute for Biotechnology (VIB). K.N. is a recipient of fellowships from the Flemish Institute for Promotion of Scientific-Technological Research and Industry (IWT). This work was supported by grants FWO-G.0136.02 (to C.A. and H.R.), Interuniversity Attraction Pole (IUAP) 120C4302 to CA and GOA 12051401 of the Concerted Research Actions of the Flemish Community to J. V and C.A.

REFERENCES

1. Pollard TD, Borisy GG. Cellular motility driven by assembly and disassembly of actin filaments. *Cell* 2003; 112:453-465.
2. Gao Y, Thomas JO, Chow RL, Lee GH, Cowan NJ. A cytoplasmic chaperonin that catalyzes beta-actin folding. *Cell* 1992; 69:1043-1050.
3. Rommelaere H, Van Troys M, Gao Y, Melki R, Cowan NJ, Vandekerckhove J, Ampe C. Eukaryotic cytosolic chaperonin contains t-complex polypeptide 1 and seven related subunits. *Proc Natl Acad Sci USA* 1993; 90:11975-11979.
4. Vainberg IE, Lewis SA, Rommelaere H, Ampe C, Vandekerckhove J, Klein HL, Cowan NJ. Prefoldin, a chaperone that delivers unfolded proteins to cytosolic chaperonin. *Cell* 1998; 93:863-873.
5. Sparrow JC, Nowak KJ, Durling HJ, Beggs AH, Wallgren-Pettersson C, Romero N, Nonaka I, Laing NG. Muscle disease caused by mutations in the skeletal muscle alpha-actin gene (ACTA1). *Neuromuscul Disord* 2003; 13:519-531.
6. Aspenstrom P, Engkvist H, Lindberg U, Karlsson R. Characterization of yeast-expressed beta-actins, site-specifically mutated at the tumor-related residue Gly245. *Eur J Biochem* 1992; 207:315-320.
7. Drummond DR, Hennessey ES, Sparrow JC. The binding of mutant actins to profilin, ATP and DNase I. *Eur J Biochem* 1992; 209:171-179.
8. Anthony Akkari P, Nowak KJ, Beckman K, Walker KR, Schachat F, Laing NG. Production of human skeletal alpha-actin proteins by the baculovirus expression system. *Biochem Biophys Res Commun* 2003; 307:74-79.

9. Georgopoulos C, Ang D. The Escherichia coli groE chaperonins. *Semin Cell Biol* 1990; 1:19-25.
10. Tian G, Vainberg IE, Tap WD, Lewis SA, Cowan NJ. Specificity in chaperonin-mediated protein folding. *Nature* 1995; 375:250-253.
11. Rommelaere H, Waterschoot D, Neiryneck K, Vandekerckhove J, Ampe C. Structural plasticity of functional actin: pictures of actin binding protein and polymer interfaces. *Structure (Camb)* 2003; 11:1279-1289.
12. Terpe K. Overview of tag protein fusions: from molecular and biochemical fundamentals to commercial systems. *Appl Microbiol Biotechnol* 2003; 60:523-533.
13. Gerdes HH, Kaether C. Green fluorescent protein: applications in cell biology. *FEBS Lett* 1996; 389:44-47.
14. Sadano H, Shimokawa-Kuroki R, Taniguchi S. Intracellular localization and biochemical function of variant beta-actin, which inhibits metastasis of B16 melanoma. *Jpn J Cancer Res* 1994; 85:735-743.
15. Lin CS, Ng SY, Gunning P, Kedes L, Leavitt J. Identification and order of sequential mutations in beta-actin genes isolated from increasingly tumorigenic human fibroblast strains. *Proc Natl Acad Sci USA* 1985; 82:6995-6999.
16. Nunoi H, Yamazaki T, Tsuchiya H, Kato S, Malech HL, Matsuda I, Kanegasaki S. A heterozygous mutation of beta-actin associated with neutrophil dysfunction and recurrent infection. *Proc Natl Acad Sci USA* 1999; 96:8693-8698.
17. Taniguchi S, Kawano T, Kakunaga T, Baba T. Differences in expression of a variant actin between low and high metastatic B16 melanoma. *J Biol Chem* 1986; 261:6100-6106.
18. Shimokawa-Kuroki R, Sadano H, Taniguchi S. A variant actin (beta m) reduces metastasis of mouse B16 melanoma. *Int J Cancer* 1994; 56:689-697.
19. Vandekerckhove J, Leavitt J, Kakunaga T, Weber K. Coexpression of a mutant beta-actin and the two normal beta- and gamma-cytoplasmic actins in a stably transformed human cell line. *Cell* 1980; 22:893-899.
20. Leavitt J, Ng SY, Varma M, Latter G, Burbeck S, Gunning P, Kedes L. Expression of transfected mutant beta-actin genes: transitions toward the stable tumorigenic state. *Mol Cell Biol* 1987; 7:2467-2476.
21. Safer D. An electrophoretic procedure for detecting proteins that bind actin monomers. *Anal Biochem* 1989; 178:32-37.
22. Laemmli UK. Cleavage of structural proteins during the assembly of the head of bacteriophage T4. *Nature* 1970; 227:680-685.
23. Schagger H, von Jagow G. Tricine-sodium dodecyl sulfate-polyacrylamide gel electrophoresis for the separation of proteins in the range from 1 to 100 kDa. *Anal Biochem* 1987; 166:368-379.
24. O'Donoghue SI, Miki M, dos Remedios CG. Removing the two C-terminal residues of actin affects the filament structure. *Arch Biochem Biophys* 1992; 293:110-116.
25. Lambrechts A, Braun A, Jonckheere V, Aszodi A, Lanier LM, Robbins J, Van Colen I, Vandekerckhove J, Fassler R, Ampe C. Profilin II is alternatively spliced, resulting in profilin isoforms that are differentially expressed and have distinct biochemical properties. *Mol Cell Biol* 2000; 20:8209-8219.
26. Pardee JD, Spudich JA. Purification of muscle actin. *Methods Cell Biol* 1982; 24:271-289.
27. Selden LA, Kinoshita HJ, Estes JE, Gershman LC. Cross-linked dimers with nucleating activity in actin prepared from muscle acetone powder. *Biochemistry* 2000; 39:64-74.
28. Hayakawa K, Ono S, Nagaoka R, Saitoh O, Obinata T. Differential assembly of cytoskeletal and sarcomeric actins in developing skeletal muscle cells in vitro. *Zoolog Sci* 1996; 13:509-517.
29. McCormack EA, Rohman MJ, Willison KR. Mutational screen identifies critical amino acid residues of beta-actin mediating interaction between its folding intermediates and eukaryotic cytosolic chaperonin CCT. *J Struct Biol* 2001; 135:185-197.
30. Asakura S. The interaction between G-actin and ATP. *Arch Biochem Biophys* 1961; 92:140-149.
31. Edgar AJ. Gel electrophoresis of native actin and the actin-deoxyribonuclease I complex. *Electrophoresis* 1989; 10:722-725.
32. Van Troys M, Dewitte D, Goethals M, Carlier MF, Vandekerckhove J, Ampe C. The actin binding site of thymosin beta 4 mapped by mutational analysis. *Embo J* 1996; 15:201-210.
33. Dedova IV, Dedov VN, Nosworthy NJ, Hambly BD, dos Remedios CG. Cofilin and DNase I affect the conformation of the small domain of actin. *Biophys J* 2002; 82:3134-3143.
34. Hansen WJ, Cowan NJ, Welch WJ. Prefoldin-nascent chain complexes in the folding of cytoskeletal proteins. *J Cell Biol* 1999; 145:265-277.
35. Rommelaere H, De Neve M, Neiryneck K, Peelaers D, Waterschoot D, Goethals M, Fraeyman N, Vandekerckhove J, Ampe C. Prefoldin recognition motifs in the nonhomologous proteins of the actin and tubulin families. *J Biol Chem* 2001; 276:41023-41028.
36. Rommelaere H, De Neve M, Melki R, Vandekerckhove J, Ampe C. The cytosolic class II chaperonin CCT recognizes delineated hydrophobic sequences in its target proteins. *Biochemistry* 1999; 38:3246-3257.
37. Nyman T, Schuler H, Korenbaum E, Schutt CE, Karlsson R, Lindberg U. The role of MeH73 in actin polymerization and ATP hydrolysis. *J Mol Biol* 2002; 317:577-589.
38. Joel PB, Fagnant PM, Trybus KM. Expression of a nonpolymerizable actin mutant in sf9 cells. *Biochemistry* 2004; 43:11554-11559.
39. Machesky LM, Hall A. Role of actin polymerization and adhesion to extracellular matrix in Rac- and Rho-induced cytoskeletal reorganization. *J Cell Biol* 1997; 138:913-926.
40. Costa CF, Rommelaere H, Waterschoot D, Sethi KK, Nowak KJ, Laing NG, Ampe C, Machesky LM. Myopathy mutations in {alpha}-skeletal-muscle actin cause a range of molecular defects. *J Cell Sci* 2004; 117:3367-3377.
41. Posern G, Sotiropoulos A, Treisman R. Mutant actins demonstrate a role for unpolymerized actin in control of transcription by serum response factor. *Mol Biol Cell* 2002; 13:4167-4178.

42. Westphal M, Jungbluth A, Heidecker M, Muhlbauer B, Heizer C, Schwartz JM, Marriott G, Gerisch G. Microfilament dynamics during cell movement and chemotaxis monitored using a GFP-actin fusion protein. *Curr Biol* 1997; 7:176-183.
43. Brault V, Sauder U, Reedy MC, Aebi U, Schoenenberger CA. Differential epitope tagging of actin in transformed *Drosophila* produces distinct effects on myofibril assembly and function of the indirect flight muscle. *Mol Biol Cell* 1999; 10:135-149.
44. Kabsch W, Vandekerckhove J. Structure and function of actin. *Annu Rev Biophys Biomol Struct* 1992; 21:49-76.
45. Schroder RR, Manstein DJ, Jahn W, Holden H, Rayment I, Holmes KC, Spudich JA. Three-dimensional atomic model of F-actin decorated with Dictyostelium myosin S1. *Nature* 1993; 364:171-174.
46. Lambrechts A, Jonckheere V, Dewitte D, Vandekerckhove J, Ampe C. Mutational analysis of human profilin I reveals a second PI(4,5)-P2 binding site neighbouring the poly(L-proline) binding site. *BMC Biochem* 2002; 3:1-12.
47. Figeys D. Novel approaches to map protein interactions. *Curr Opin Biotechnol* 2003, 14:119-125.
48. Kabsch W, Mannherz HG, Suck D, Pai EF, Holmes KC. Atomic structure of the actin: DNase I complex. *Nature* 1990; 347:37-44.
49. Schutt CE, Myslik JC, Rozycki MD, Goonesekere NC, Lindberg U. The structure of crystalline profilin-beta-actin. *Nature* 1993; 365:810-816.
50. Holmes KC, Popp D, Gebhard W, Kabsch W. Atomic model of the actin filament. *Nature* 1990; 347:44-49.
51. Leavitt J, Ng SY, Aebi U, Varma M, Latter G, Burbeck S, Kedes L, Gunning P. Expression of transfected mutant beta-actin genes: alterations of cell morphology and evidence for autoregulation in actin pools. *Mol Cell Biol* 1987; 7:2457-2466.
52. Sakai Y, Okamoto H, Mogami K, Yamada T, Hotta Y. Actin with tumor-related mutation is antimorphic in *Drosophila* muscle: two distinct modes of myofibrillar disruption by antimorphic actins. *J Biochem (Tokyo)* 1990; 107:499-505.
53. Drummond DR, Hennessey ES, Sparrow JC. Characterisation of missense mutations in the Act88F gene of *Drosophila melanogaster*. *Mol Gen Genet* 1991; 226:70-80.
54. Wertman KF, Drubin DG, Botstein D. Systematic mutational analysis of the yeast ACT1 gene. *Genetics* 1992; 132:337-350.
55. Olson TM, Michels VV, Thibodeau SN, Tai YS, Keating MT. Actin mutations in dilated cardiomyopathy, a heritable form of heart failure. *Science* 1998; 280:750-752.
56. Olson TM, Doan TP, Kishimoto NY, Whitby FG, Ackerman MJ, Fananapazir L. Inherited and de novo mutations in the cardiac actin gene cause hypertrophic cardiomyopathy. *J Mol Cell Cardiol* 2000; 32:1687-1694.
57. van Wijk E, Krieger E, Kemperman MH, De Leenheer EM, Huygen PL, Cremers CW, Cremers FP, Kremer H. A mutation in the gamma actin 1 (ACTG1) gene causes autosomal dominant hearing loss (DFNA20/26). *J Med Genet* 2003; 40:879-884.
58. Zhu M, Yang T, Wei S, DeWan AT, Morell RJ, Elfenbein JL, Fisher RA, Leal SM, Smith RJ, Friderici KH. Mutations in the gamma-actin gene (ACTG1) are associated with dominant progressive deafness (DFNA20/26). *Am J Hum Genet* 2003; 73:1082-1091.
59. Schagger H, von Jagow G. Blue native electrophoresis for isolation of membrane protein complexes in enzymatically active form. *Anal Biochem* 1991; 199:223-231.

PROTOCOLS

Protocol 1: In vitro transcription/translation

| | |
|--|---------------|
| Reticulocyte lysate (Promega) | 12.5 μ l |
| TNT-buffer | 1 μ l |
| T7 polymerase | 0.5 μ l |
| Amino acids minus methionine | 0.5 μ l |
| ³⁵ S-methionine (10 mCi/ml ICN) | 2.8 μ l |
| RNAguard RNase inhibitor (Amersham Biosciences) | 0.5 μ l |
| RNA-Cap structure analogue (m ⁷ G(5')ppp(5')G, New England Biolabs) | 0.5 μ l |
| ATP (50 mM) | 0.5 μ l |
| MgCl ₂ (10 mM) | 1.25 μ l |
| H ₂ O/buffer* | 4.4 μ l |
| DNA (+/- 200 ng/ μ l) | 2 μ l |
| Total volume | 26.45 μ L |

All reagents should be RNase free and sterile.

Add all reagents and let react for 1h30 at 30°C. Analyse or store at -80°C till further use.

*H₂O is recommended by the manufacturer. We found that a mixture of water and buffer containing 50 mM KCl, 5 mM MgCl₂, 1mM EGTA, 20 mM MES pH6.8 and 1 mM DTT in a 2/3 ratio results in higher expression levels than adding water alone.

Protocol 2: Native and denaturing gels

A) Native gels

The dimensions of the gels we make are 9 × 8 cm × 0.5 mm (0.75 mm in the case of Hansen gels) and we use slots that can contain 15 to 20 μ l. It is very important that the gels are prerun and run at 4°C, higher temperatures cause in most cases aggregation.

1. Safer gels (21)

Gel composition for two gels:

| | 4.5 % | 7.5 % | 10 % |
|-----------------------------|-------------|-------------|-------------|
| 1M TRIS | 250 μ l | 250 μ l | 250 μ l |
| 1M glycine | 1.94 ml | 1.94 ml | 1.94 ml |
| 30% acrylamide | 1.5 ml | 2.5 ml | 3.3 ml |
| 2% bis-acrylamide | 0.6 ml | 1.0 ml | 1.3 ml |
| H₂O | 5.5 ml | 4.1 ml | 3.0 ml |
| 100mM ATP (optional) | 20 μ l | 20 μ l | 20 μ l |
| 10 % APS | 100 μ l | 100 μ l | 100 μ l |
| TEMED | 10 μ l | 10 μ l | 10 μ l |

Running buffer:

25 mM Tris (3.025 g/l), 194 mM glycine (14.55 g/l), 0.2 mM ATP (2 ml 100 mM, if required).
The final pH at 4°C will be 8.7 (adjusting the pH is not necessary). Store at 4°C.

5X loading buffer:

50% running buffer, 50% glycerol, spatula point bromophenol blue. In the case of reticulocyte lysate this buffer is not added.

Running conditions:

prerun: 1h at 4°C and 175 V (to bring the gel at pH 8.7).

run : +/- 1h at 4°C and 175 V (till the haemoglobin has reached one third of the gel or till the bromophenol blue has run off). Time may vary depending on the pI of the proteins to analyse.

2. MES gels (2)

Gel composition:

| 4.5 % | 3 gels |
|--|----------|
| 30% acrylamide; 0.8% bis-acrylamide | 2.25 ml |
| 1M MES (pH 6.7) | 1.2 ml |
| 500 mM EGTA (pH 7.5) | 30 µl |
| 1 M MgCl₂ | 15 µl |
| H₂O | 11.25 ml |
| 100 mM ATP (optional) | 160 µl |
| 100 mM GTP (optional) | 160 µl |
| 10% APS | 100 µl |
| TEMED | 20 µl |

Running buffer: 80 mM MES/KOH pH 6.7 (80 ml 1 M), 1 mM MgCl₂ (1 ml 1 M), 1 mM EGTA (2 ml 500 mM), 0.1 mM ATP (1 ml 100 mM, if required) for 1 liter. Store at 4°C. It is important to use tanks that can contain sufficient amounts of buffer (e.g. approximately 300 ml and 200 ml in the upper and lower tank, respectively) to avoid warming up of the system, and to avoid pH-changes. Sometimes it's necessary to renew the buffers during the run.

2X Loading buffer: 50% running buffer, 50% glycerol, spatula point bromophenol blue.

Running conditions:

prerun: 1h at 4°C and 100V.

run: 100 V at 4°C until 15 min after bromophenol blue ran off the gel.

3. Discontinue gradient native gels according to Hansen *et al.* (34, 59)

Gel composition for four gels:

| | 13 % separation | 6 % stacking |
|--|-----------------|--------------|
| H₂O | 6.6 ml | 11.4 ml |
| 48 % acrylamide; 1.5 % bis-acrylamide | 4.7 ml | 2.5 ml |
| 1.5 M 6-aminocaproic acid; 150 mM BisTris, pH 7 | 6 ml | 7 ml |
| Glycerol | 3.6 ml | |
| 10% APS | 60 µl | 90 µl |
| TEMED | 6 µl | 9 µl |

Running buffers:

Anode buffer (+, lower chamber): 50 mM BisTris, pH 7 (10.4 g/l)

Cathode buffer (-, upper chamber): 50 mM Tricine (8.95 g/l), 15 mM BisTris (3.135 g/l), pH 7

2X loading buffer: 100 mM BisTris pH 7, 10 % glycerol, 4 mM glutathione, 2 mM methionine, 2 mM cysteine and spatula point Ponceau S.

Running conditions: 20 min at 50 V (\pm 5 mA) at 4°C, remaining time at 13 mA (\pm 150 V) till red front reaches the bottom of the gel.

B) Denaturing Gels

Gel composition for 3 gels:

| | 10% separation | 4% stacking |
|--|----------------|-------------|
| 48 % Acrylamide; 1.5 % bis-acrylamide | 3.05 ml | 1.0 ml |
| 3M Tris; 0.3 % SDS; pH 8.45 | 5.0 ml | 3.1 ml |
| 87 % glycerol | 1.87 ml | -- |
| H₂O | 5.0 ml | 8.24 ml |
| APS | 75 μ l | 95 μ l |
| TEMED | 7.5 μ l | 25 μ l |

Running buffer:

Anode buffer (+, lower chamber): 0.2 M Tris pH 8.3 (24.3 g/l).

Cathode buffer (-, upper chamber): 0.1 M Tris pH 8.25 (12.11g/l), 0.1 M Tricine (17.92 g/l),

0.1 % SDS (5 ml 20%) (no pH adjustment necessary).

5X loading buffer (1 ml): 200 μ l 20% SDS, 24% glycerol, 50 μ l 1M Tris-HCl pH 6.8, 20 μ l β -mercapto-ethanol, 490 μ l H₂O, spatula point bromophenol blue.

C) Treatment of gels after running

Disassemble everything and stain the gel with Coomassie blue for 5 min. Handle the 4.5% gels with a lot of care, they break very easily, it is best to put the plate with the gel in the staining chamber and peel the gel carefully of. Destain for 15 min. Incubate the gel for 15 min in Amplify solution (Amersham). Put the gel on Saran wrap, and cover it with a piece of Whatman paper (1 mm). This assembly is then dried at 80°C in a gel dryer for 30 min. After drying the Saran wrap is peeled of and the gel can be fluorographed.

Protocol 3: Copolymerization assay (Fig. 2A)

1. Perform an *in vitro* transcription translation reaction of wild type or mutant β -actin in a total volume of 26.45 μ l (see protocol 1). After reaction, remove 1 μ l and add it to 3 μ l 2X Laemmli buffer for analysis to check for expression of the protein.
2. Centrifuge the remaining 25 μ l at 100 000 rpm in a Beckman airfuge to pellet aggregates
3. Transfer the supernatant to a second airfuge tube. Add 50 μ l 1X Laemmli buffer to the tube with aggregates for analysis.
4. To the supernatant, add 25 μ l of 12 μ M α -actin (purified from rabbit skeletal muscle according to Pardee *et al.*, (26)) in G-buffer (2 mM TrisHCl, pH 8, 0.2 mM CaCl₂, 0.5 mM DTT, 0.2 mM ATP) and mix by pipetting up and down.
5. Add 1.6 μ l 3M KCl and 0.5 μ l 100 mM MgCl₂ (= F-buffer conditions).
6. Allow to polymerise for 2 hours at room temperature
7. Pellet the actin filaments by centrifugation at 100 000 rpm for 20 minutes (= pellet 1).
8. Remove the supernatant (= sn1, 50 μ l) that contains the unpolymerized actin and add 3 μ l 5X Laemmli buffer for analysis.
9. Gently wash pellet 1 with G-buffer.

10. Resuspend pellet 1 in 80 μ l G-buffer by pipetting carefully up and down.
11. Allow depolymerising overnight at 4°C. Although not performed here, residual filaments can be removed by centrifugation at 100 000 rpm for 20 minutes before induction of the second round of polymerization
12. Induce a second round of polymerization by adding 1.6 μ l 3M KCl and 0.5 μ l 100 mM MgCl₂, let polymerise for 2 hours at room temperature.
13. Pellet actin filaments by airfuge centrifugation at 100 000 rpm for 20 minutes (= pellet 2).
14. Remove the supernatant (=sn2, 80 μ l) and add 3 μ l 5X Laemmli buffer for analysis.
15. Pellet 2 is dissolved in 50 μ l Laemmli buffer.
16. Analyse 2 μ l of the aggregates, 2 μ l of sn1, 10 μ l of sn2 and 10 μ l of pellet 2 on 12.5% SDS-gels (see Fig. 6). The Coomassie stain of the gel shows in which fraction the carrier actin is retained (mostly in pellet 2, in case of capping activity, in the supernatants).
17. Quantify the amount of ³⁵S-labeled actin in each fraction using phosphor imaging and the ImageQuant software package.
18. To determine the total amount of ³⁵S-labeled actin, multiply the amount for the aggregates by 5, for sn1 by 26.5, for sn2 by 8.3 and for pellet 2 by 5, and sum all these values.
19. The % of actin in each fraction is the total amount in each fraction divided by the total amount.